Physics Letters B 293 (1992) 226–236
North-Holland

PHYSICS LETTERS B

Prompt photon energy spectra in B-decays and determination of the CKM matrix elements

A. Ali
Deutsches Elektronen Synchrotron – DESY, W-2000 Hamburg, FRG

and

C. Greub [1]
Universität Zürich, CH-8001 Zurich, Switzerland

Received 10 July 1992

We present theoretical estimates of the inclusive prompt photon energy spectrum in direct decays of B-hadrons through the charged current processes $B\to X_c+\gamma$ and $B\to X_u+\gamma$, and the flavour changing neutral current (FCNC) processes $B\to X_s+\gamma$ and $B\to X_d+\gamma$ (here the subscript q on X_q denotes the quark flavour in the transition $b\to q$). It is argued that the various components in the inclusive spectrum can, in principle, be disentangled using the photon energy and flavour tagging the hadron(s) recoiling against the photon in B-decays, thereby providing a new technique to determine the CKM matrix elements $|V_{cb}|$, $|V_{ub}|$, $|V_{ts}|$, and $|V_{td}|$. In particular, the high energy part of the inclusive photon energy spectrum being dominated by the electromagnetic penguins could provide the first direct measurement of the CKM matrix element $|V_{ts}|$. We quantify this by firming up predictions for the inclusive decays $B\to X_s+\gamma$ in the standard model.

1. Introduction

Semileptonic B-decays have provided valuable information on the properties of the b-quark, in particular the Cabibbo–Kobayashi–Maskawa (CKM) [1] matrix elements $|V_{cb}|$ and $|V_{ub}|$ [2]. In this paper, we focus on radiative B-decays. We present a first estimate of the inclusive photon energy spectrum in the decays $B\to X+\gamma$. With a high-resolution electromagnetic calorimeter and large enough B-meson sample, it should be possible to measure the prompt (hard) photon radiation spectrum in the weak decays of heavy quarks. Quite importantly, precision measurements of the inclusive and exclusive photon energy spectra in B-decays may provide new techniques to determine the CKM matrix elements. We elaborate this point on the example of the decay $B\to X_s+\gamma$ which would determine the CKM matrix element $|V_{ts}|$.

To get the inclusive photon spectra in $B\to X+\gamma$, both the charged current (CC) radiative transitions $B\to(X_c, X_u)+\gamma$, involving the basic couplings in the SM lagrangian [3], and the flavour changing neutral current (FCNC) processes $B\to(X_s, X_d)+\gamma$, induced by the so-called electromagnetic penguins, have to be taken into account. The former decays are sensitive to the CKM matrix elements $|V_{cb}|$ and $|V_{ub}|$ as can be seen in table 1, where the dominant CC transitions at the quark level are listed together with their CKM matrix element dependence. The FCNC radiative decays $B\to(X_s, X_d)+\gamma$, on the other hand, are essentially determined by the magnetic moment operators, whose Wilson coefficients are dominated by the top quark contribution in the processes $b\to(s, d)+\gamma+(g)$. This brings to the fore the dependence of the rates of the top quark mass (m_t) and the CKM matrix elements $|V_{ts}|$ (for $B\to X_s+\gamma$) and $|V_{td}|$ (for $B\to X_d+\gamma$) [4,5]. It follows that a precise measurement of the prompt photon energy spectra in B decays has, in principle, the potential of determin-

[1] Partially supported by Schweizerischer Nationalfonds.

Table 1
CC radiative b-quark decays contributing to $B\to(X_c, X_u)+\gamma$ and their CKM matrix element dependent factors K_n.

n	Reaction	K_n
1	$b\to c\,d\bar{u}\gamma$	$3\lvert V_{cb}\rvert^2\lvert V_{ud}\rvert^2$
2	$b\to c\,d\bar{c}\gamma$	$3\lvert V_{cb}\rvert^2\lvert V_{cd}\rvert^2$
3	$b\to c\,s\bar{u}\gamma$	$3\lvert V_{cb}\rvert^2\lvert V_{us}\rvert^2$
4	$b\to c\,s\bar{c}\gamma$	$3\lvert V_{cb}\rvert^2\lvert V_{cs}\rvert^2$
5	$b\to c\,e^-\bar{\nu}\gamma$	$\lvert V_{cb}\rvert^2$
6	$b\to c\,\mu^-\bar{\nu}\gamma$	$\lvert V_{cb}\rvert^2$
7	$b\to c\,\tau^-\bar{\nu}\gamma$	$\lvert V_{cb}\rvert^2$
8	$b\to u\,d\bar{u}\gamma$	$3\lvert V_{ub}\rvert^2\lvert V_{ud}\rvert^2$
9	$b\to u\,d\bar{c}\gamma$	$3\lvert V_{ub}\rvert^2\lvert V_{cd}\rvert^2$
10	$b\to u\,s\bar{u}\gamma$	$3\lvert V_{ub}\rvert^2\lvert V_{us}\rvert^2$
11	$b\to u\,s\bar{c}\gamma$	$3\lvert V_{ub}\rvert^2\lvert V_{cs}\rvert^2$
12	$b\to u\,e^-\bar{\nu}\gamma$	$\lvert V_{ub}\rvert^2$
13	$b\to u\mu^-\bar{\nu}\gamma$	$\lvert V_{ub}\rvert^2$
14	$b\to u\,\tau^-\bar{\nu}\gamma$	$\lvert V_{ub}\rvert^2$

ing the four CKM matrix elements: $|V_{cb}|$, $|V_{ub}|$, $|V_{ts}|$, and $|V_{td}|$. We calculate the components of interest of the inclusive photon energy spectrum in B-decays, taking into account the B-meson wave function effects consistently in both the CC and FCNC sectors, using the experimental constraints from the inclusive lepton energy spectrum in semileptonic B-decays. Summing up the four components provides the inclusive photon energy spectrum in $B\to X+\gamma$.

The immediate interest in such a measurement, however, lies in the high-frequency part of the photon spectrum since it is a sensitive probe of the FCNC electromagnetic penguins in B-decays. With an eye on the imminent developments in this field, in particular from the CLEO Collaboration [6], we revisit the decays $B\to X_s+\gamma$ by taking into account the dependence of the rates and photon energy spectrum on the various parameters of the underlying theoretical framework. In particular, we focus on the inclusive branching ratio $BR(B\to X_s+\gamma)$ and calculate the bounds on the CKM matrix element $|V_{ts}|$, that would follow from the experimental measurement of this quantity.

The paper is organized as follows. In section 2, we discuss the calculations of the matrix elements for the CC transitions leading to the photon energy spectra in the decays $b\to(c, u)+Y+\gamma$, where Y denotes a quark–antiquark or lepton pair. We also specify the essential features of the B-meson wave function model that we have used to get the photon energy spectra from the decays $B\to(X_c, X_u)+\gamma$ and $B\to(X_s, X_d)+\gamma$. Section 3 summarizes the calculations for the FCNC decays $B\to X_s+\gamma$ and $B\to X_d+\gamma$ [4,5]. The resulting branching ratios for the decays $B\to X_s+\gamma$ and $B\to X_d+\gamma$ and their dependence on the various parameters, including the CKM matrix elements, top quark mass, and the renormalization scale are also presented here. Finally, in section 4 we summarize the main features of the inclusive photon energy spectra presented in this paper. An estimate of the exclusive branching ratio $BR(B\to K^*+\gamma)$ is also given here.

2. CC radiative B-decays

The CC radiative decays $B\to X_c+\gamma$ and $B\to X_u+\gamma$ that we want to calculate are modelled after the quark decays given in table 1. They represent single photon bremsstrahlung processes from all the charged fermion lines (leptons and quarks) evaluated in the spectator model. Note that we have neglected the so-called W-exchange two-body decays, since they are generally considered negligible in B-decays [7]. Also, there is no compelling evidence in the experiments calling for a revision of this opinion. The most convincing support in favour of the dominance of the spectator model contribution is the (near) equality of the charged- and neutral B-meson lifetimes, gotten indirect through the ARGUS and CLEO measurements of the semileptonic branching ratios [8]:

$$\frac{\tau_{B^\pm}}{\tau_{B^0}}=\frac{BR(B^\pm\to D^{(*)0}\ell^\pm\nu)}{BR(B^0\to D^{(*)-}\ell^+\nu)}=0.96\pm0.14\,. \qquad (1)$$

We now specify the approximations used in calculating the inclusive photon energy spectrum from the CC processes. First, we have left out the QCD corrections to the decays listed in table 1. It is to be noted here that the renormalization group improvements of the effective four-Fermi interactions are known from analogous studies in the non-radiative B-decays and they could have been included without much ado. These improvements are, however, numerically not important [7,9,10]; also they represent only a part of the corrections. It is to be noted that the radiative semileptonic decays contribute more significantly to the CC radiative B-decays due to the smallness of the

electron and muon mass. Hence, the dominant (and non-trivial) corrections in CC decays are expected to arise from the leading QCD contribution to the semileptonic radiative decays, including real and virtual gluon bremsstrahlung processes such as $b\to(c,u)\ell\nu_\ell+\gamma+g$, which, as far as we know, are not yet calculated. These corrections will be needed as the experimental precision on the inclusive photon energy measurements improve. For a first estimate, the CC processes listed in table 1 are quite adequate. However, it is well known that the QCD corrections to the electromagnetic penguins in the decays $b\to(s,d)+\gamma$ are very important [11]. We of course keep these correction, both real and virtual, in the evaluation of the FCNC radiative decays $B\to(X_s, X_d)+\gamma$ along the lines described in refs. [4,5].

We have also left out the QED virtual corrections to the processes in table 1, as a result of which our calculations are ill-suited to describe the soft photon energy spectrum in radiative B-decays. There is no experimental interest in the soft photon spectrum either, since it is inundated by the initial state radiation (in e^+e^- production processes) and secondary photons from the pion and kaon decays produced in B-decays and in background processes. Depending on the experimental details, the photon energy spectrum above a certain threshold (say $E_\gamma \geqslant 1.0$ GeV in the B-rest frame) should, however, be reliably given by the sum of the CC contributions in table 1 and the FCNC contributions discussed in the next section. With these remarks, we now proceed to outline the derivation of the inclusive photon energy spectrum in B-decays.

We define the kinematics of the CC radiative B-decays on the example of reaction $n\equiv 1$ in table 1,

$$b(p_1)\to c(p_2)+d(p_3)+\bar{u}(p_4)+\gamma(k)\,. \tag{2}$$

The fully differential decay width for a b quark decaying at rest reads as

$$d\Gamma_n \equiv \frac{(2\pi)^4}{2m_b}\delta^4(p_1-p_2-p_3-p_4-k) \times\overline{|M_n|^2_\Sigma}\,d\mu(p_2)\,d\mu(p_3)\,d\mu(p_4)\,d\mu(k)\,, \tag{3}$$

where the sum over the final spin and colour factors and average over the initial spin and colour are implied. The symbol $d\mu(p)$ defines the invariant measure for each particle in the final state, $d\mu(p)=d^3p/(2\pi)^3 2p^0$. The spin- and colour-averaged matrix element squared can be expressed as

$$\overline{|M_n|^2_\Sigma} = 128\pi\alpha_{em}G_F^2|A|^2K_n\,. \tag{4}$$

Here K_n is a reaction dependent factor given in table 1 and the reduced matrix element squared $|A|^2$ is given below:

$$\begin{aligned}|A|^2 &= 2p_2\cdot p_3\left(\frac{Q_1^2}{p_1\cdot k}p_4\cdot k+\frac{Q_4^2}{p_4\cdot k}p_1\cdot k\right)\\ &+2p_1\cdot p_4\left(\frac{Q_2^2}{p_2\cdot k}p_3\cdot k+\frac{Q_3^2}{p_3\cdot k}p_2\cdot k\right)\\ &-4(Q_2Q_3\,p_1\cdot p_4-Q_1Q_4\,p_2\cdot p_3)\\ &-p_2\cdot p_3\left(\frac{Q_1}{p_1\cdot k}+\frac{Q_4}{p_4\cdot k}\right)(B\cdot p_4\,p_1\cdot k-B\cdot p_1\,p_4\cdot k)\\ &-p_1\cdot p_4\left(\frac{Q_2}{p_2\cdot k}-\frac{Q_3}{p_3\cdot k}\right)(B\cdot p_3\,p_2\cdot k-B\cdot p_2\,p_3\cdot k)\\ &-\tfrac{1}{2}B\cdot B p_2\cdot p_3\,p_1\cdot p_4\,,\end{aligned} \tag{5}$$

with

$$B^\mu = 2\left(\frac{Q_1\,p_1^\mu}{p_1\cdot k}-\frac{Q_2\,p_2^\mu}{p_2\cdot k}-\frac{Q_3\,p_3^\mu}{p_3\cdot k}+\frac{Q_4\,p_4^\mu}{p_4\cdot k}\right), \tag{6}$$

and Q_i are the electric charges of the fermions. For the non-leptonic radiative decays (reactions 1–4 and 8–11 in table 1), they have the values $Q_1=Q_3=-\frac{1}{3}$, $Q_2=Q_4=+\frac{2}{3}$, while for the semileptonic decays (reactions 5–7 and 12–14 in table 1), they have the values $Q_1=-\frac{1}{3}$, $Q_2=+\frac{2}{3}$, $Q_3=-1$, $Q_4=0$. To get the photon energy spectra from these processes, the integration over the phase space has been done using a Monte Carlo programme. To avoid the collinear region which, due to the smallness of m_e, is accentuated in the semileptonic decay involving the electron, $b\to(u,c)e\bar{\nu}_e+\gamma$, one could put a cone around the electron direction and exclude the $(\gamma+e)$ collinear configuration. With the matrix element given in (5), this can be done for a given experimental setup. For the sake of this paper, we set the electronic radiative decay width equal to the muonic. We have compared the photon energy spectra in the CC b-quark transitions with the corresponding ones obtained in ref. [12] and we are in agreement with their results. To get the photon energy spectrum from the B-hadron decays, however, one has to incorporate the wave

function effects. The resulting CC spectra will be presented after we have described the wave function model being used.

The B-meson wave function model as applied to the FCNC decays is discussed in refs. [4,5]. This model has previously been used in the derivation of inclusive semileptonic distributions [13,14], where it is known to give a good description of the measured lepton energy spectrum. In this model the b-quark is given a non-zero momentum having a gaussian distribution represented by an a priori free (but adjustable) parameter, p_F:

$$\phi(p)=\frac{4}{\sqrt{\pi}p_F^3}\exp\left(\frac{-p^2}{p_F^2}\right),\quad p=|\boldsymbol{p}|\,. \tag{7}$$

The energy-momentum constraint is imposed in the form

$$W^2=M_B^2+m_q^2-2M_B\sqrt{p^2+m_q^2}\,, \tag{8}$$

where M_B is the B-meson mass, W, the effective mass of the b-quark, and m_q, the mass of the spectator quark in the B-meson, $B=b\bar{q}$. The mass of the decaying b-quark varies according to eq. (8). The photon energy spectrum from the decay of the B-meson at rest is then given by

$$\frac{d\Gamma}{dE_\gamma}=\int_0^{p_{max}}\phi(p)p^2\,dp\,\frac{d\Gamma_b}{dE_\gamma}(W,p,E)\,, \tag{9}$$

where $\phi(p)$ is normalized as

$$\int_0^\infty\phi(p)p^2\,dp=1\,, \tag{10}$$

p_{max} is the maximum allowed value of p, and $d\Gamma_b/dE_\gamma$ is the photon energy spectrum from the decay of the b-quark in flight, having a mass W and momentum p. This can be obtained by Lorentz boosting the b-quark decay spectrum at rest. The physical kinematic threshold in the problem and the energy–momentum constraint eq. (8) have to be respected. The dependence of the inclusive rates for both $B\to X_d+\gamma$ and $B\to X_s+\gamma$ on the wave-function parameter, p_F, is negligible, though the photon energy spectra, very much like the lepton energy spectra in semileptonic B decays, are sensitive to its value. We take the best fit for p_F obtained from a fit of the ARGUS and CLEO inclusive lepton energy spectrum $p_F=0.30\pm0.09$ GeV [15,16]. The branching ratio for the both the CC and FCNC radiative decays are calculated using the total B-decay width, Γ_{tot}:

$$\Gamma_{tot}=(r_u|V_{ub}|^2+r_c|V_{cb}|^2)\Gamma_0\,,$$

$$\Gamma_0=\frac{W_{eff}^5G_F^2}{192\pi^3}\,,\quad r_u\approx7\,,\quad r_c\approx3\,. \tag{11}$$

The values of r_u and r_c include phase space and QCD corrections [7,17]. The dependence on the effective b-quark mass, W_{eff}, which enters as the fifth power in both Γ_{tot} and all the radiative decays considered here cancels to a very large extent in the respective branching ratios. Note that the spectra and all the decay rates are calculated directly in terms of the B-meson mass. The effective b-quark mass, entering in Γ_{tot}, can also be expressed in terms of the B-meson mass and the parameter p_F. A very good (numerical) functional dependence of W_{eff} for the present model can be parametrized as

$$W_{eff}^2\simeq M_B^2-2M_B\cdot p_F\cdot1.28\,. \tag{12}$$

In the numerical estimates, a number of quark and lepton masses and the CKM matrix elements are needed. For the CKM matrix, we always use the Wolfenstein parametrization [18]. The explicit form of this matrix and an update of the actual values of the CKM matrix elements can be seen in ref. [19]. Unless stated otherwise, the parameters used in our analysis are listed in table 2, and the others are taken from the PDG tables [20].

The inclusive photon energy spectra from the CC

Table 2
List of parameters and their default values used in the numerical estimates of the B-decay rates and photon energy spectra.

Parameter	Default value
m_t (GeV)	140
m_c (GeV)	1.68
m_s (GeV)	0.50
$m_u=m_d$ (GeV)	0.30
μ (GeV)	5.0
$\Lambda^{(5)}$ (GeV)	0.225
p_F (GeV)	0.3
$\|V_{ts}\|$	0.041
$\|V_{cb}\|$	0.041
$\|V_{ub}\|/\|V_{cb}\|$	0.14
$\|V_{cd}\|=\|V_{us}\|$	0.220
$\|V_{cs}\|=\|V_{ud}\|$	0.975

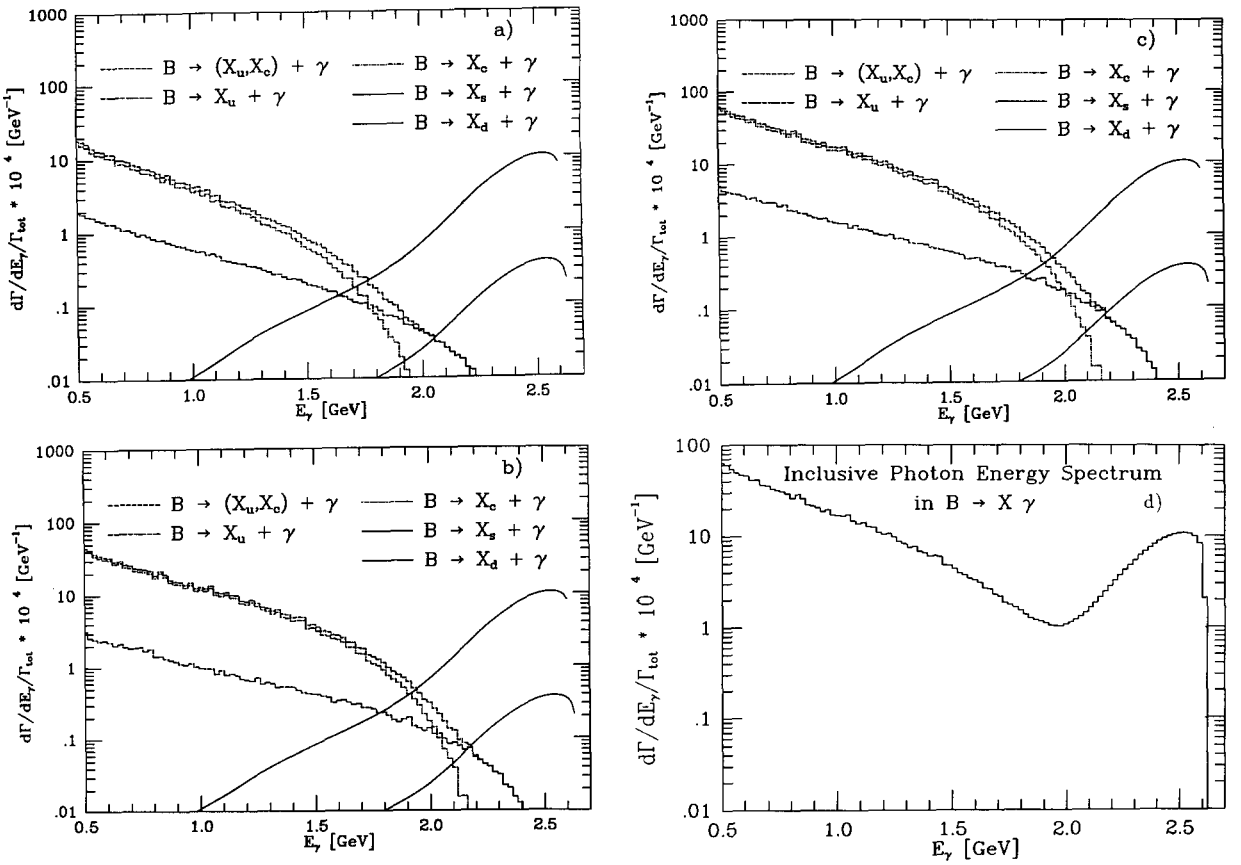

Fig. 1. Inclusive photon energy spectra from the CC decays $B\to(X_c, X_u)+\gamma$, their sum, and the corresponding spectra from the FCNC decays $B\to X_s+\gamma$ and $B\to X_d+\gamma$. (a) Including only the semileptonic CC radiative decays given in table 1, (b) including only the non-leptonic CC decays in table 1, (c) including all the CC decays in table 1, (d) the inclusive photon energy spectrum in the decays $B\to X+\gamma$ obtained by summing up the spectra in (c).

radiative decays including the B-meson wave function effects are plotted in figs. 1a–1c, corresponding to the non-leptonic decays, semileptonic decays and their sum, respectively. In each of these figures, we show the contribution from the decays $B\to X_c+\gamma$, $B\to X_u+\gamma$ and their sum $B\to(X_c, X_u)+\gamma$, as well as the contribution from the FCNC processes $B\to X_s+\gamma$ and $B\to X_d+\gamma$ (discussed in the next section). We postpone a discussion of these spectra to section 4.

3. FCNC decays $B\to X_s+\gamma$ and $B\to X_d+\gamma$

We have already reported the calculations leading to the inclusive branching ratios for the FCNC decays $B\to X_s+\gamma$ and $B\to X_d+\gamma$, and the resulting inclusive photon energy spectra in a series of papers [4,5]. Since these papers are sufficiently detailed, we will restrict ourselves to recalling the salient features of this work necessary for the discussion here. We recall that the inclusive rates and spectra have been calculated in the framework of an effective theory with five quarks, obtained by integrating out the heavier degrees of freedom (top quark and $W^{\pm}$ bosons), by keeping only the operators with the lowest (mass) dimensions. To leading order in the small (weak)-mixing angles, a complete set of dimension-six operators relevant for the processes $b\to s+\gamma$ and $b\to s+\gamma+g$ is contained in the effective hamiltonian

$$H_{\rm eff}(b\to s\gamma) = -\frac{4G_F}{\sqrt{2}}\lambda_t \sum_{j=1}^{8} C_j(\mu)\hat{O}_j(\mu)\,, \qquad (13)$$

where G_F is the Fermi coupling constant, $C_j(\mu)$ are the Wilson coefficients evaluated at the scale μ, and $\lambda_t = V_{tb}V_{ts}^*$, with V_{ij} being the Cabibbo–Kobayashi–Maskawa (CKM) matrix elements. Note that the operators $\hat{O}_1, ..., \hat{O}_6$ are the four-fermion operators, and $\hat{O}_7$ and $\hat{O}_8$ are the QED and QCD magnetic moment operators, respectively. Their definitions, matching conditions $C_i(m_W)$, and the leading log perturbative QCD corrections giving $C_i(\mu)$ with $\mu \ll m_W$ can be seen in ref. [11]. We use the definitions and estimates of $C_i(\mu)$ from Grinstein et al. in ref. [11]. Discussing the contribution of the bremsstrahlung diagrams $b\to s+\gamma+g$, we recall that the diagrams associated with $\hat{O}_1$ vanish due to the colour structure. Also, the coefficient of the operator $\hat{O}_8$ gets suppressed after including QCD effects and its contribution can be neglected. The operators $\hat{O}_3, ..., \hat{O}_6$ get contribution only from operator mixing and are also numerically unimportant. Thus, the dominant contribution to $B\to X_s+\gamma$ are due to the operators $\hat{O}_2$ and $\hat{O}_7$ (the electromagnetic penguin operator) which are defined as

$$\hat{O}_2 = (\bar{c}_{L\alpha}\gamma^\mu b_{L\alpha})(\bar{s}_{L\beta}\gamma_\mu c_{L\beta})\,,$$
$$\hat{O}_7 = (e/16\pi^2)\bar{s}_\alpha \sigma^{\mu\nu}(m_b R + m_s L) b_\alpha F_{\mu\nu}\,,$$
$$L = \tfrac{1}{2}(1-\gamma_5)\,, \quad R = \tfrac{1}{2}(1+\gamma_5)\,. \qquad (14)$$

Here e denotes the QED coupling constant. The coefficients $C_2(\mu)$, $C_7(\mu)$, obtained in the leading logarithm approximation (LLA) [11], and the corresponding coefficients at the scale m_W are listed below:

$$C_2(\mu) = \tfrac{1}{2}(\eta^{-6/23} + \eta^{12/23})C_2(m_W)\,,$$
$$C_7(\mu) = \eta^{-16/23}[C_7(m_W) - \tfrac{58}{135}(\eta^{10/23}-1)C_2(m_W)$$
$$- \tfrac{29}{189}(\eta^{28/23}-1)C_2(m_W)]\,,$$
$$C_2(m_W) = 1\,,$$
$$C_7(m_W) = F_2(x)\,, \qquad (15)$$

with $\eta = \alpha_s(\mu)/\alpha_s(m_W)$ being the ratio of the QCD coupling constants and $x = m_t^2/m_W^2$. The Inami–Lim function $F_2(x)$ derived from the penguin diagrams is given by [21]

$$F_2(x) = \frac{x}{24(x-1)^4}[6x(3x-2)\log x$$
$$-(x-1)(8x^2+5x-7)]\,. \qquad (16)$$

It is clear from eqs. (13), (15), (16) that a measurement of the inclusive branching ratio for $B\to X_s+\gamma$ provides information on $|V_{ts}|$ and m_t, given other parameters. Before we quantify this information there is one point, however, which we would like to stress here concerning the renormalization scale dependence of the QCD-improved Wilson coefficients in $H_{\rm eff}$ defined above. We recall here that the coefficients $C_i(\mu)$ given in eq. (15), being LLA results, show a significant dependence on the renormalization scale μ. In the decays of B-hadrons, the b-quark mass suggests itself as a natural choice, i.e. $\mu = m_b$, which is what has been used in the literature to determine the decay rates in $b\to s+\gamma$ [11]. However, it is difficult to pin down the scale μ that sharply. It is prudent to allow μ to vary within some reasonable range. Following this argument, we shall vary μ in the range $m_b/2 \leqslant \mu \leqslant 2m_b$. As we shall see this is one of the dominant uncertainties in the electromagnetic penguin amplitudes.

The modifications that have to be implemented for the CKM-suppressed FCNC radiative decays $b\to d+\gamma$ and $b\to d+\gamma+g$ have been discussed in ref. [5]. We recall here that for the decays $b\to s+\gamma(+g)$ the effective hamiltonian was written in the approximation where the CKM factor $\lambda_u = 0$, which is reasonable since $\lambda_u \ll (\lambda_c, \lambda_t)$ (where $\lambda_i \equiv V_{ib}V_{is}^*$). For the decays $b\to d+\gamma$ and $b\to d+\gamma+g$ the CKM factors λ_i are replaced by $\xi_i \equiv V_{ib}V_{id}^*$. Now ξ_u, ξ_c and ξ_t are all of the same order of magnitude. In the Wolfenstein parametrization [18], one has $\xi_i = O(\lambda^3)$, where $\lambda = \sin\theta_C = 0.22$. Hence, the corresponding approximation $\xi_u = 0$ cannot be made any longer. The differences due to the inclusion of ξ_u to describe the decays $b\to d+\gamma$ and $b\to d+g+\gamma$ can be most easily built in the effective hamiltonian framework by modifying the operators $\hat{O}_1$ and $\hat{O}_2$, encountered in the decay $b\to s+\gamma$. The dimension-six operator basis again reads as

$$H_{\rm eff}(b\to d\gamma) = -\frac{4G_F}{\sqrt{2}}\xi_t \sum_{j=1}^{8} C_j(\mu)O_j(\mu)\,. \qquad (17)$$

The operators O_1 and O_2 are defined as

$$O_1 = -\frac{\xi_c}{\xi_t}(\bar{c}_{L\beta}\gamma^\mu b_{L\alpha})(\bar{d}_{L\alpha}\gamma_\mu c_{L\beta}) - \frac{\xi_u}{\xi_t}(\bar{u}_{L\beta}\gamma^\mu b_{L\alpha})(\bar{d}_{L\alpha}\gamma_\mu u_{L\beta}),$$

$$O_2 = -\frac{\xi_c}{\xi_t}(\bar{c}_{L\alpha}\gamma^\mu b_{L\alpha})(\bar{d}_{L\beta}\gamma_\mu c_{L\beta}) - \frac{\xi_u}{\xi_t}(\bar{u}_{L\alpha}\gamma^\mu b_{L\alpha})(\bar{d}_{L\beta}\gamma_\mu u_{L\beta}). \quad (18)$$

With the operators defined in this basis, the matching conditions, $C_i(m_W)$, and the corresponding Wilson coefficients at the scale μ, $C_i(\mu)$, are precisely the same for the decays $b\to d+\gamma$ as given earlier for the $b\to s+\gamma$ case. Also, for the decays $b\to d+\gamma+g$ only the contributions associated with O_2 and O_7 are important. However, in the diagrams associated with O_2 both u- and c- quark propagate in the loop. This is an important difference in comparison to the $b\to s+\gamma+g$ case, where there is perfect cancellation in the charm quark and top quark contributions for the loop-momenta below the charm mass threshold. In the decays $b\to d+\gamma+g$, this cancellation is upset due to the non-vanishing contribution of the u-quark, though the contribution from the low momentum region in the loop is numerically small. We shall see later that the long-distance contribution to the FCNC decays $B\to X_d+\gamma$, modelled after the CC decays given in table 1, is also numerically small, in particular, in the high frequency part of the photon spectrum. We maintain, though we cannot rigorously prove it, that the FCNC decays $B\to X_d+\gamma$, very much like their dominant counterparts, $B\to X_s+\gamma$, are also short-distance dominated.

The inclusive branching ratio for $B\to X_d+\gamma$ depends on m_t and μ through the Wilson coefficients $C_i(\mu)$, and on the CKM parameters ρ and η which enter through the CKM factors ξ_t and ξ_c. In the Wolfenstein parametrization these read as

$$\xi_t = A\lambda^3(1-\rho+i\eta), \quad \xi_c = -A\lambda^3. \quad (19)$$

This specifies the theoretical framework; we now discuss the inclusive branching ratios for the decays $B\to X_s+\gamma$ and $B\to X_d+\gamma$ and their dependence on the various input parameters. The default values of the parameters used in the numerical estimates for the CC and FCNC branching ratios and energy spectra are given in table 2. We shall vary some of these parameters and discuss their effect below. First of all, the masses of the light quarks, m_u, m_d and m_s are numerically not important and we fix them to their default values given in table 2. The contribution of the charm quark enters through the loop in the diagrams for the decays $b\to(s, d)+\gamma+g$. This dependence is again not very sensitive to the precise value of m_c, but we shall include the effect of its variation in the range $1.3\leqslant m_c\leqslant 1.7$ GeV. The b-quark mass in our approach is not a free parameter. Its value is fixed by the B-hadron mass and the Fermi motion parameter p_F, discussed earlier. The branching ratios for $B\to X_s+\gamma$ and $B\to X_d+\gamma$ depend on m_t, though unfortunately not crucially, as will be shown below. We vary m_t in the presently favoured range from the electroweak phenomenology $m_t = 140\pm 40$ GeV [22]. For the scale dependence of the strong coupling constant, which is needed for the estimates of the rates and spectra for the FCNC decays $B\to(X_s, X_d)+\gamma$, we use the two loop β function

$$\alpha_s(\mu) = \frac{12\pi}{(33-2N_f)\log(\mu^2/\Lambda^2)} \times\left(1-\frac{6(153-19N_f)}{(33-2N_f)^2}\frac{\log\log(\mu^2/\Lambda^2)}{\log(\mu^2/\Lambda^2)}\right). \quad (20)$$

We set $N_f=5$ and the corresponding $\Lambda^{(5)}=225$ MeV, which is the central value from a recent compilation [23]. The dependence of the branching ratio $BR(B\to X_s+\gamma)$ on m_t and μ is shown in fig. 2, where it is plotted as a function of μ with the upper curve corresponding to $m_t=180$ GeV and the lower to $m_t=100$ GeV. Based on this figure, a firm prediction for this branching ratio in the SM is

$$BR(B\to X_s+\gamma) = (2\text{–}5)\times 10^{-4}. \quad (21)$$

This range is somewhat larger than $BR(B\to X_s+\gamma) = (3\text{–}4)\times 10^{-4}$, given in ref. [4], as we have now included the dependence of the branching ratio on the scale μ. As can be seen in fig. 2, the m_t dependence of $BR(B\to X_s+\gamma)$ in the assumed m_t-range is only O(25%). It would, therefore, be difficult to extract a meaningful bound on m_t from a measurement of $BR(B\to X_s+\gamma)$. We remark that the central value in fig. 2, $BR(B\to X_s+\gamma)=3.5\times 10^{-4}$ (corresponding to $\mu=5.0$ GeV and $m_t=140$ GeV), is not too far away

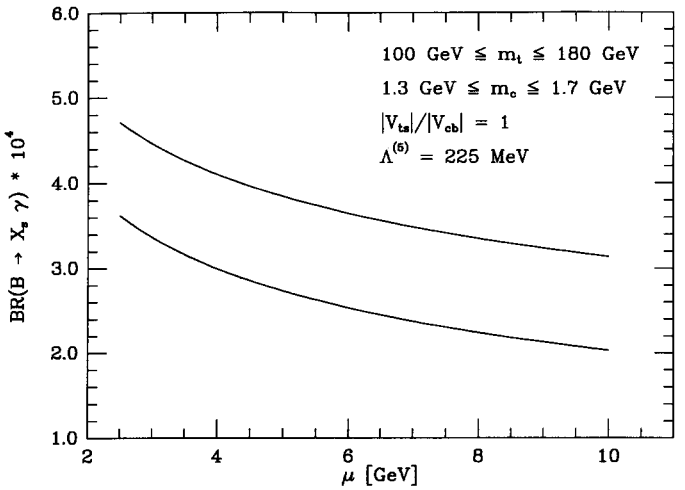

Fig. 2. Inclusive branching ratio $BR(B\to X_s+\gamma)$ as a function of the renormalization scale μ, with the upper curve corresponding to $m_t=180$ GeV and the lower to $m_t=100$ GeV. The other parameters used in the analysis are shown in the figure.

from the present (conservative) bound on this branching ratio, namely $BR(B\to X_s+\gamma)<9.0\times 10^{-4}$ (at 90% CL) [6]; hence a measurement in this channel is in the wings!

While confirming the branching ratio in (21) will constitute a non-trivial test of the SM in the flavour sector, one could ask more ambitiously what would be the main thrust of an eventual measurement of $BR(B\to X_s+\gamma)$? We maintain, that the overriding theoretical interest in the study of electromagnetic penguins in B-decays lies in the direct measurement of the CKM matrix elements $|V_{ts}|$ and $|V_{td}|$ (more precisely ρ and η). To that end, we show the dependence of the branching ratio $B\to X_s+\gamma$ on the CKM ratio $(|V_{ts}|/|V_{cb}|)^2$ in fig. 3, where all the other sensitive parameters are varied within the indicated ranges. The unitarity bounds on the ratio of the CKM matrix elements $0.25\leqslant(|V_{ts}|/|V_{cb}|)^2\leqslant 4.0$ [20] are implicitly included in fig. 3. We remark that, despite considerable uncertainties in the theoretical estimates, a measurement of the inclusive branching ratio for $B\to X_s+\gamma$ can provide a non-trivial bound on the CKM matrix element $|V_{ts}|$. For the sake of clarifying the potential strength of an eventual measurement of $BR(B\to X_s+\gamma)$, we note that a *hypothetical value* $BR(B\to X_s+\gamma)=(4\pm 1)\times 10^{-4}$ would imply $0.80\leqslant|V_{ts}|/|V_{cb}|\leqslant 1.60$, i.e. a determination of $|V_{ts}|$ to better than a factor 2.

Finally, the decay rates for $B\to X_d+\gamma$ depend on the CKM parameters ρ and η which enter through the CKM factors ξ_t and ξ_c, as already discussed. Numerically, we put $\lambda=0.22$, $A=0.847$ (in agreement with the numerical value for $|V_{cb}|$) and vary the parameters (ρ,η), in a consistent way to satisfy all the phenomenological constraints from x_d, $|V_{ub}|/|V_{cb}|=0.14\pm 0.05$ and ϵ_K, using $m_t=140\pm 40$ GeV. This gives the following range [5]:

$$BR(B\to X_d+\gamma)=(0.8\text{–}4)\times 10^{-5}. \qquad (22)$$

For $m_t=140$ GeV and $\mu=5$ GeV, this range is somewhat reduced giving $BR(B\to X_d+\gamma)=(1.0\text{–}3.0)\times 10^{-5}$. In the calculation of the photon energy spectrum for $B\to X_d+\gamma$ shown in fig. 1, we have used the value $(\rho,\eta)=(0.2, 0.4)$, the central value obtained from the fits of the data for $m_t=140$ GeV in ref. [5].

4. Inclusive photon energy spectrum in $B\to X+\gamma$

The inclusive photon energy spectra from the FCNC decays $B\to X_s+\gamma$ and $B\to X_d+\gamma$ are shown in fig. 1. Since these spectra were calculated by us in refs. [4,5] with the same approximations and parameter values as used here, we refer to these papers for details. Following observations concerning figs. 1a–1d are in order.

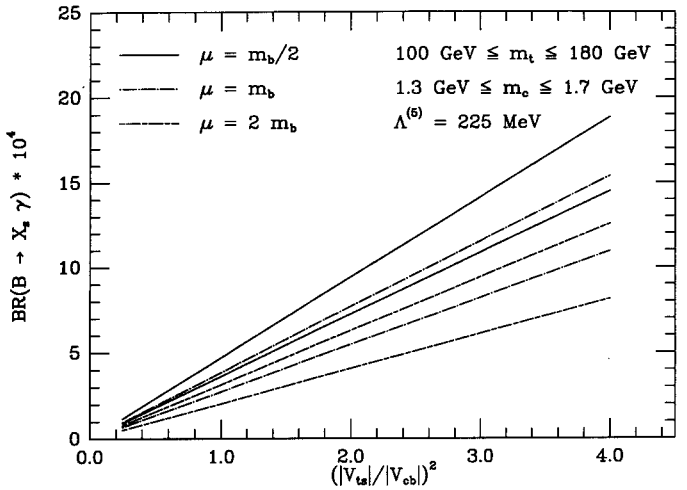

Fig. 3. Inclusive branching ratio BR(B→$X_s+\gamma$) as a function of the CKM matrix element ratio $(|V_{ts}|/|V_{cb}|)^2$, with the indicated range of the various parameters. Each value of μ leads to the allowed band, and the three indicated bands correspond to $\mu=\frac{1}{2}m_b$, m_b, and $2m_b$.

– The inclusive photon energy spectrum in the decays B→X+γ, shown in fig. 1d, divides itself in three regions. The first is the low frequency part $E_\gamma \leqslant 1.8$ GeV, which is dominated by the CC decay B→$X_c+\gamma$, a small intermediate region $1.9 \leqslant E_\gamma \leqslant 2.1$ GeV, where the CC and FCNC contributions are comparable, and the high frequency part $E_\gamma \geqslant 2.1$ GeV, which is dominated by the FCNC radiative decay B→$X_s+\gamma$. Precise measurements of the photon energy spectra in these regions can therefore be used to test the normalization and shape of the two dominating components. The dip in fig. 1d in the region $E_\gamma = (1.9-2.0)$ GeV has an obvious origin.

– The significantly different thresholds in the two CC radiative transitions, due to the presence of a charmed hadron in the decays B→$X_c+\gamma$ versus non-charmed light hadrons in B→$X_u+\gamma$, result in the longer E_γ-tail for the latter. However, in the region where the photons from the dominant CC process B→$X_c+\gamma$ range out (say above 2 GeV in the B rest frame), the inclusive photon spectrum is dominated by the CKM allowed FCNC radiative decay B→ $X_s+\gamma$.

– The separation of the high frequency part of the spectrum in the two FCNC components B→$X_s+\gamma$ and B→$X_d+\gamma$ would require flavour tagging the hadrons recoiling against the photon, for example, by demanding the overall strangeness quantum number of X_d being 0 and X_s being equal to ± 1. At the exclusive level, this can be exemplified by the decays B→K*+ $(n\pi)+\gamma$ versus B→ρ+ $(n\pi)+\gamma$.

– Our calculations also indicate that the long distance (i.e. CC) contamination to the short distance piece (i.e. penguin dominated FCNC decays) is small in the high energy region of the photon spectrum. This is a rather important conclusion, since otherwise the final states in the CC radiative decays B→$X_u+\gamma$ and the FCNC decays B→$X_d+\gamma$ very easily mock up each other.

– This analysis also demonstrates that probably the most difficult to measure is the CC component B→ $X_u\rightarrow\gamma$, since there is no region in which it dominates. The only way to isolate this component is probably through the measurement of the photon spectrum in the low frequency part and demanding the absence of charmed hadrons in B→X+γ, recoiling against the photon. With a vertex detector, perhaps this is feasible in a limited range of photon energy, though the non-B-background will be formidable, perhaps prohibitive.

Finally, one could use the inclusive photon energy spectrum in B→$X_s+\gamma$, given in fig. 1, combined with the assumption of K*-dominance of the hadron mass spectrum in the limited kinematic domain $(m_K + m_\pi) \leqslant m_X \leqslant 1.0$ GeV to estimate the exclusive branching ratio BR(B→K*+γ), as was done in ref.

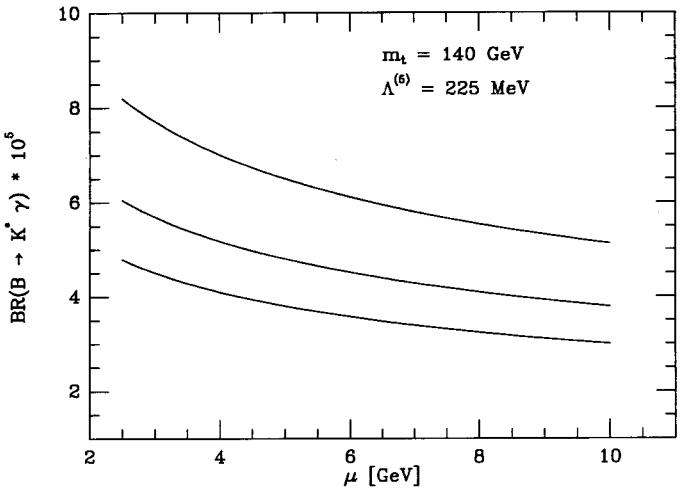

Fig. 4. Inclusive branching ratio BR(B→K*+γ) as a function of the renormalization scale μ. The three curves correspond to p_F=0.21 GeV (top), p_F=0.30 GeV (central), and p_F=0.39 GeV (bottom), and the other parameters are given in table 2.

[4]. Since one of the new ingredients of the present analysis is the dependence of the branching ratios on the renormalization scale, we show this dependence for BR(B→K*+γ) in fig. 4. The three curves correspond to p_F=0.21 GeV (top), p_F=0.30 GeV (central), and p_F=0.39 GeV (bottom), and the other parameters are given in table 2. This gives the following prediction:

$$BR(B\to K^*+\gamma)=(3\text{–}8)\times 10^{-5}\,, \qquad (23)$$

to be compared with the present experimental bound [6]: BR(B→K*+γ) < 9.0×10^{-5} (at 90% CL). This mode therefore should be seen soon, though the interpretation of the data in this case is model dependent. This, in our model, is exemplified by the p_F-dependence of BR(B→K*+γ) shown through the three curves in fig. 4. We recall that the inclusive branching ratios for B→X_s+γ and B→X_d+γ do not depend on p_F (more generally on the wave function model) and hence are more predictive.

The measurement of the inclusive photon energy spectrum in B-decays would be a benchmark measurement opening up new experimental opportunities using prompt photons in heavy quark weak decays. We hope that the calculations presented here are useful in the interpretation of data on radiative B-decays, in particular concerning the electromagnetic penguins.

Acknowledgement

We acknowledge a helpful discussion with Michael Shifman.

References

[1] N. Cabibbo, Phys. Rev. Lett. 10 (1963) 531;
M. Kobayashi and K. Maskawa, Prog. Theor. Phys. 49 (1973) 652.
[2] A. Ali, DESY report 91-137 (1991); in: B Decays, ed. S. Stone (World Scientific, Singapore, 1992).
[3] S.L. Glashow, Nucl. Phys. 22 (1961) 579;
S. Weinberg, Phys. Rev. Lett. 19 (1967) 1264;
A. Salam, in: Elementary particle theory, ed. N. Svartholm (Almqvist and Wiksell, Stockholm, 1968).
[4] A. Ali and C. Greub, Z. Phys. C 49 (1991) 431; Phys. Lett. B 259 (1991) 182.
[5] A. Ali and C. Greub, Phys. Lett. B 287 (1992) 191.
[6] G. Eigen (CLEO Collab.), DESY Seminar (June 1992).
[7] G. Altarelli and S. Petrarca, Phys. Lett. B 261 (1991) 303.
[8] H. Schröder, in: QCD – 20 years later (Aachen, June, 1992).
[9] G. Altarelli and L. Maiani, Phys. Lett. B 52 (1974) 351;
M.K. Gaillard and B.W. Lee, Phys. Rev. Lett. 33 (1974) 351.

[10] G. Altarelli et al., Phys. Lett. B 99 (1981) 141; Nucl. Phys. B 187 (1981) 461;
A.J. Buras and P.H. Weisz, Nucl. Phys. B 333 (1990) 66;
A.J. Buras et al., MPI-München report MPI-PAE/PTh 56/91 (1991).
[11] S. Bertolini, F. Borzumati and A. Masiero, Phys. Rev. Lett. 59 (1987) 180;
R. Grigjanis et al., Phys. Lett. B 213 (1988) 355;
B. Grinstein, M.J. Savage and M.B. Wise, Nucl. Phys. B 319 (1989) 271;
B. Grinstein, R. Springer and M.B. Wise, Nucl. Phys. B 339 (1990) 269;
G. Cella et al., Phys. Lett. B 248 (1990) 181;
M. Misiak, Phys. Lett. B 269 (1991) 161.
[12] G. Eilam, R. Mendel and R. Migneron, Z. Phys. C 52 (1991) 145.
[13] A. Ali and E. Pietarinen, Nucl. Phys. B 154 (1979) 519.
[14] G. Altarelli, M. Cabibbo, G. Corbo, L. Maiani and G. Martinelli, Nucl. Phys. B 208 (1982) 365.
[15] CLEO Colab., R. Fulton et al., Phys. Rev. Lett. 64 (1990) 16;
S. Stone, private communication.
[16] ARGUS Collab., H. Albrecht et al., Phys. Lett. B 234 (1990) 409; B 249 (1990) 359.
[17] A. Paschos and U. Türke, Phys. Rep. 178 (1989) 145.
[18] L. Wolfenstein, Phys. Rev. Lett. 51 (1983) 1945.
[19] A. Ali and D. London, DESY report 92-075 (1992), J. Phys. G, to appear.
[20] Particle Data Group, J.J. Hernández et al., Review of particle properties, Phys. Lett. B 239 (1990) 1.
[21] T. Inami and C.S. Lim, Progr. Theor. Phys. 65 (1981) 297.
[22] J. Carter, Proc. Intern. Lepton–photon Symp. and Europhysics Conf. on High energy physics, eds., S. Hegerty, K. Potter and E. Quercigh (Geneva, 1991).
[23] G. Altarelli, in: QCD – 20 years later (Aachen, June, 1992).
[24] A. Ali, DESY report DESY 92-058 (1992).